

for the Ch_D and Ch_{BX} , respectively. The existence of the second-order band already observed in the nematic phases^{8,13} seems to indicate that at a microscopic scale, the nematic pseudolamellar order¹³ is maintained in the cholesteric phases. Also, the continuous increase of s_1^{-1} for increasing temperatures is analogous to previous experiments in nematic phases.¹³ These results indicate that in the Ch_{BX} phase the long axes of the biaxial micelles are oriented parallel to the helicoidal axis (the two other orthogonal axes twist from one nematic plane to another).

Concluding Remarks

The observation of only one cholesteric pitch in Ch_{BX} (with or without \vec{H}) in our experimental conditions is remarkable. "A priori" three different pitches could be expected in this phase, corresponding to the twist along the three independent twofold symmetry axes of the local biaxial system. In this case without \vec{H} , a defect lattice typical of a blue phase¹⁰ would have been observed. But such a network of line defects costs energy. This may explain that, even very close to the Ch_{BX} transitions, the system prefers to twist only one axis (directed along the long axis of the micelles) and to untwist the two other directions. Recently,

(13) Figueiredo Neto, A. M.; Galerne, Y.; Levelut, A. M.; Liébert, L. J. *Phys. Lett.* **1985**, *46*, L-499.

a phase of this type has been predicted and described theoretically.¹⁴ In this case, the biaxial cholesteric and the uniaxial cholesteric (which in fact is also locally biaxial¹⁵) have the same symmetry. As first noticed by Brand and Pleiner,¹⁶ such a cholesteric to cholesteric transition similar to the liquid-gas transition cannot be of second order. Since the transitions between the three cholesteric phases look perfectly continuous under all our observations, we may conclude that, either the transitions are weakly first order for small concentrations of BS and our techniques are not sensitive to detect it, or they are not really phase transitions as the liquid-gas transition above the critical point.

Acknowledgment. We thank Drs. A. M. Levelut, H. Pleiner, and H. R. Brand for helpful discussions. We gratefully acknowledge the donors of Petroleum Research Fund, administered by the American Chemical Society, for financial support of this work.

Registry No. NadS, 151-21-3; decanol, 112-30-1; brucine sulfate, 4845-99-2.

(14) Pleiner H.; Brand, H. R., submitted for publication.

(15) Yaniv, Z.; Vaz, N. A. P.; Chidichimo, G.; Doane, J. W. *Phys. Rev. Lett.* **1981**, *47*, 46.

(16) Brand, H. R.; Pleiner, H., submitted for publication.

Investigation of the Quasi-Liquid Crystal Structure

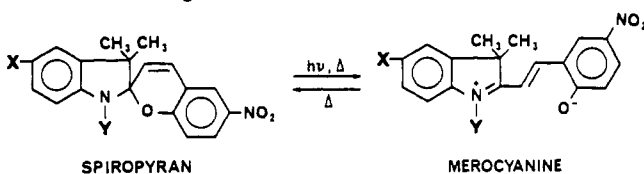
Felix P. Shvartsman, Ivan R. Cabrera, Alexander L. Weis,[†] Ellen J. Wachtel,[†] and Valeri A. Krongauz*

Department of Structural Chemistry, The Weizmann Institute of Science, Rehovot 76100, Israel
(Received: April 1, 1985)

Quasi-liquid crystals, a metastable mesophase of thermochromic spiropyrans containing mesogenic groups, were investigated by different methods. Miscibility studies, X-ray diffraction, and UV-visible and FT-IR spectroscopy indicate that the material behaves basically as a nematic mesophase. Comparison of data of the present work with that obtained earlier by optical and ESR investigation of the behavior of fluorescent and paramagnetic probes results in the formulation of a structural model for quasi-liquid crystals.

Introduction

Spiropyrans are among the most extensively investigated organic photo- and thermochromes.¹ The color changes are associated with the following reversible reactions:²



Earlier we observed different types of molecular assemblies, formed on conversion of spiropyrans into merocyanine dyes.³⁻⁸ The assemblies are based on the capability of the merocyanine dyes or spiropyran-merocyanine complexes to form giant molecular stacks.⁹

Recently we have reported a new type of structural organization for spiropyran-merocyanine systems, quasi-liquid crystals (QLCs), obtained from spiropyrans containing mesogenic groups.^{10,11} Crystals of these spiropyrans ($X = RPhCOOPhCH=N-$; $Y = CH_3-$) melt into isotropic liquid. However, metastable amorphous films of these compounds prepared by fast evaporation of the solvent from their solution give a birefringent texture upon heating.

Appearance of texture, characteristic of a mesophase, coincides with a sharp increase in the merocyanine concentration, resulting in a color change of the films from yellow to green, due to thermochromic spiropyran \rightarrow merocyanine conversion. Further increase in temperature leads to the disappearance of texture but it appears again upon cooling. The temperature range of the birefringent texture is rather wide (for example, spiropyran with $R = CH_3O-$ has a texture between 50-130 °C) and lies much

(1) Bertelson, R. C. "Photochromism"; Brown, G. H., Ed.; Wiley: New York, 1971; Chapter 3.

(2) Fischer, E.; Hirschberg, Y. *J. Chem. Soc.* **1952**, 4522.

(3) Krongauz, V. A.; Fishman, S. N.; Goldburt, E. S. *J. Phys. Chem.* **1978**, *82*, 2469.

(4) Meredith, G. R.; Williams, D. J.; Fishman, S. M.; Goldburt, E. S.; Krongauz, V. A. *J. Phys. Chem.* **1983**, *87*, 1697.

(5) Krongauz, V. A.; Goldburt, E. S. *Macromolecules* **1981**, *14*, 1382.

(6) Goldburt, E. S.; Shvartsman, F. P.; Krongauz, V. A. *Macromolecules* **1984**, *17*, 1876.

(7) Goldburt, E. S.; Shvartsman, F. P.; Fishman, S. N.; Krongauz, V. A. *Macromolecules* **1984**, *17*, 1225.

(8) Cabrera, I. R.; Shvartsman, F. P.; Veinberg, O. N.; Krongauz, V. A. *Science* **1984**, *226*, 341.

(9) Sturmer, D. M.; Heseltine, D. W. In "The Theory of the Photographic Process," Jammes, H., Ed.; MacMillan: New York, 1977; Chapters 7 and 8.

(10) Shvartsman, F. P.; Krongauz, V. A. *Nature (London)* **1984**, *309*, 608.

(11) Shvartsman, F. P.; Krongauz, V. A. *J. Phys. Chem.* **1984**, *88*, 6448.

[†] Department of Organic Chemistry.

* Department of Polymer Research.

below the melting point of the spirogyran crystals ($\sim 200^\circ\text{C}$). The mesophase is not monotropic.

The quasi-liquid crystalline films crystallize with time. The films can be aligned in an electrostatic field of more than 0.5 kV/mm. The alignment of the films stabilizes the quasi-liquid crystalline state and spontaneous crystallization no longer occurs. Under supercooled conditions at room temperature the mesophase with homogeneous alignment is preserved practically indefinitely.

The electronic absorption spectra of the QLC films showed that only a small part of the material (around 5%) is in the colored, merocyanine form. Examination of the films aligned in the electrostatic field revealed that only in the visible region of the spectrum, corresponding to merocyanine absorption, did the linear dichroism differ appreciably from zero (order parameter $S \sim 0.4$). In the UV region, corresponding to the absorption of the bulk comprised of spirogyran molecules, linear dichroism was not distinguishable from zero. However, under a polarizing microscope one can see a rather good alignment of the bulk. We tried to explain this inconsistency by assuming that spirogyran molecules are arranged in ordered domains with a structure similar to that of the axially symmetric micelles in lyotropic liquid crystals.^{10,11} The merocyanine molecules may promote formation of the spirogyran domains that can be considered as solvating shells around the dye dipoles.

In principle, the merocyanine molecules may simply serve as dichroic dye probes, being intercalated in, and indicating the order parameter of, the liquid crystalline host. Other dye molecules, both polar (4-(dimethylamino)-4'-nitrostilbene, DANS) and nonpolar (1,6-diphenylhexatriene, DPH), added to QLC films are aligned in the field as well. The fact that the order parameter found for the polar probe ($S \sim 0.5$) is about twice as large as for the nonpolar ($S \sim 0.22$) is consistent with the assumption that polar dye molecules play an active role in formation of the mesophase.

A nitroxide free radical (*p-n*-octylbenzoyloxyperdeuterio-2,2,6,6-tetramethylpiperidine-1-oxyl) was used as a paramagnetic probe for ESR studies of the supercooled aligned QLC films. The ESR spectrum represents a superposition of two components, one of which is invariant upon sample orientation, while the other alters upon reorientation of the sample in the magnetic field.¹²

Partition of the probe between two sites of the QLC matrix was assumed: site I is associated with the isotropic ESR spectrum and site II is associated with the spectrum dependent on sample orientation. Two-component simulation of the ESR spectrum led us to the conclusion that the partition of the probe between two sites is roughly equal. In site II the probe strongly interacts with the matrix and the order parameter was found to be 0.33. If a micellar-like structure for QLCs was assumed the hypothesis that the additives reside in between the micelles, rather than being located at their center, is more consistent with the ESR data. Furthermore, there was uncertainty in comparing the order parameters measured by electronic absorption and emission spectroscopy and by ESR: the first two methods imply that the probe is distributed uniformly in the bulk and give the net order parameter for the whole QLC phase, while ESR gives the value only for the anisotropic site II.

In order to define the QLC structure we undertook more systematic studies of this material including examination of miscibility with other liquid crystals, X-ray diffraction, polarization IR, and UV-visible spectroscopy. Most experiments were conducted with the compound with $R = \text{CH}_3\text{O}^-$. We compare all the available data in an attempt to develop a more consistent picture.

Experimental Section

Chemicals. *p*-Nitrophenylhydrazine (Fluka), methyl isopropyl ketone (BDH), 4-methoxybenzoic acid (BDH), 4-hydroxybenzaldehyde (BDH), di-*tert*-butyl dicarbonate (Fluka), *p*-(*p*-ethoxyphenylazo)phenyl crotonate (Kodak), and *N*-tetra-

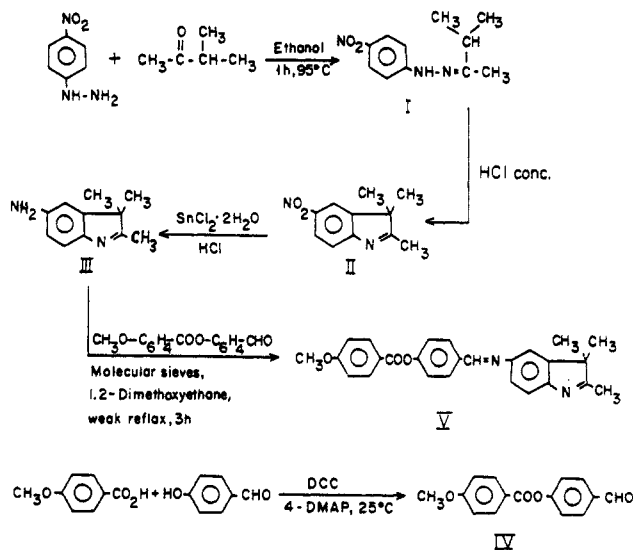


Figure 1. Reaction scheme for the synthesis of MBTI.

phthaldehyde-bis(4-*n*-butylaniline) (Kodak) were used without further purification.

Syntheses. 5-(4'-Methoxybenzoyloxy)benzylidenamino-2,3,3-trimethylindolenine (MBTI, V) was synthesized as shown in Figure 1. Melting points given below are not corrected.

The *p*-nitrophenylhydrazone (I) was prepared by heating of equivalent amounts of hydrazine and ketone.¹³

5-Nitro-2,3,3-indolenine (II) was obtained by cyclization of I according to the method described in ref 14.

Reduction of II by the procedure described in ref 15 gave 5-amino-2,3,3-trimethylindolenine (III). Crystallization of the product from hexane:benzene (1:4) gave needlelike yellow crystals, mp $185\text{--}186^\circ\text{C}$ in a yield of 94%. Anal. Calcd for $\text{C}_{11}\text{H}_{14}\text{N}_2$: C, 75.23; H, 8.10; N, 16.08. Found: C, 75.35; H, 8.09; N, 16.06.

4-(4'-Methoxybenzoyloxy)benzaldehyde (IV) was synthesized by direct esterification¹⁶ of 4-methoxybenzoic acid with 4-hydroxybenzaldehyde at room temperature. The yield of white crystals was 80%, mp $83\text{--}85^\circ\text{C}$. Anal. Calcd for $\text{C}_{15}\text{H}_{12}\text{O}_4$: C, 70.31; H, 4.72. Found: C, 70.33; H, 4.75.

5-(4'-Methoxybenzoyloxy)benzylidenamino-2,3,3-trimethylindolenine (V) was prepared by weak reflux of solution of III and IV in dry 1,2-dimethoxyethane in the presence of freshly activated molecular sieves as a dehydrating agent according to the method A given in ref 17. The yield of V after crystallization from benzene:hexane 1:2 was 76% (yellow crystals). Anal. Calcd for $\text{C}_{26}\text{H}_{24}\text{N}_2\text{O}_3$: C, 75.71; H, 6.35; N, 6.79. Found: C, 75.44; H, 6.41; N, 6.82.

5-(4'-Methoxybenzoyloxy)benzylidenamino-1,3,3-trimethyl-6'-nitrospiro(indoline-2,2'(2*H*)-1)-benzopyran (MBIS) was obtained as it was described in ref 11 (the stereo formula is shown in Figure 8).

Differential Scanning Calorimetry (DSC). Preparation of the samples for DSC measurements was similar to the preparation of the QLC films for optical measurements: benzene solutions of MBIS or MBTI or their mixtures were dropped onto the bottom of an aluminum pan heated to 80°C for calorimetric measurements. After evaporation of the solvent the amount of material in each pan was approximately 2 mg. After the material was cooled and sealed, the pan was placed in the chamber of a Mettler TA3000 DSC calorimeter. The scan speed of the heating runs was $10^\circ\text{C}/\text{min}$.

X-ray Diffraction. The MBTI sample was prepared by melting crystals in a 1-mm-diameter X-ray capillary and then fast cooling

(13) Schofield, K.; Theobald, R. *J. Chem. Soc.* **1949**, 796.

(14) Deorha, D.; Joshi, S. *J. Org. Chem.* **1968**, *26*, 3527.

(15) Gale, D. J.; Wilshire, J. F. K. *J. Soc. Dyers Colour* **1974**, *90*, 97.

(16) Hassner, A.; Alexanian, V. *Tetrahedron Lett.* **1978**, *46*, 4475.

(17) Orahovats, A. S.; Radeva, T. Zh.; Spassov, S. L. *C. R. Acad. Bulg. Sci.* **1973**, *26*, 663.

(12) Meirovitch, E.; Shvartsman, F. P.; Krongauz, V. A.; Zimmermann, H. *J. Phys. Chem.*, in press.

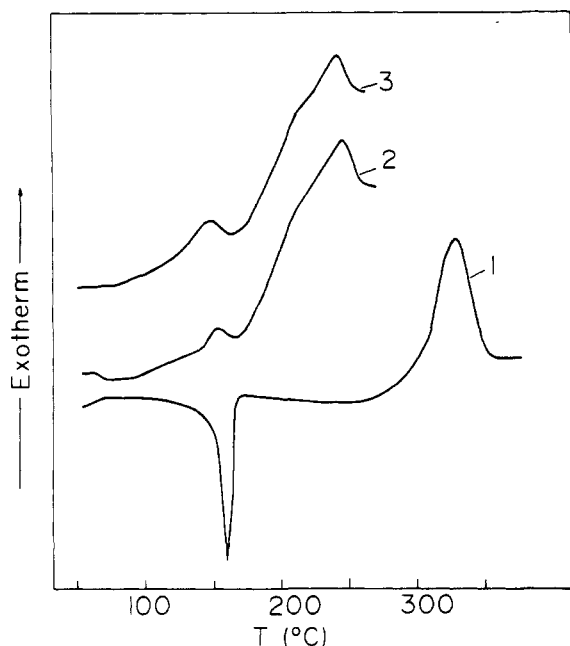


Figure 2. DSC thermograms: (1) MBTI; (2) 3:2 MBIS:MBTI; (3) 2:3 MBIS:MBTI.

the mesophase. The MBIS samples for X-ray measurements were prepared on the surface of mica according to the procedure described in ref 10.

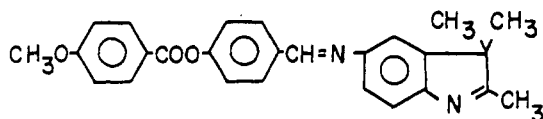
Diffraction profiles were measured on a Searle camera with Franks optics adapted for use with a one-dimensional position-sensitive detector.¹⁸ The detector window was 1 mm × 10 cm and the distance from the sample to the detector anode was 7.8 cm. Data were accumulated for 1 h and histogrammed in a Z-80 based microprocessor. The X-ray generator was an Elliott GX6 fitted with a 200- μ m focus cap, operating at 39 kV and 28 mA. Helium flushed the sample chamber.

Optical Measurements. A polarizing microscope (Wild 8M) with Ernst Leitz Wetzlar hot stage was used for macroscopic observations. A spectrophotometer (Varian 2200) was employed for UV-visible absorption measurements. The infrared (IR) polarization absorption spectra were measured on a Nicolet MX-1 Fourier transform infrared (FT-IR) spectrometer with linear polarization attachment.

The aligned QLC films for IR polarization spectra were prepared according to the procedure described earlier¹⁰ on a NaCl prism, bearing vacuum-deposited gold electrodes.

Results and Discussion

Phase Transitions of MBTI. In order to understand the role of the benzopyran portion of a quasi-liquid crystalline molecule in the formation of the mesophase, we investigated the mesophase of MBTI.



Yellow crystals of MBTI, when melted, give a mesophase in the range 160–326 °C; above this temperature the mesophase disappears with a sharp change of color from orange-yellow to dark brown, and with an exothermic, apparently chemical transformation of the material (Figure 2).

The mesophase displays a focal-conic fan texture, characteristic of a smectic A phase (S_A).¹⁹ It gives homeotropic texture easily, and uncovered droplets show "steps" or "terraces" along their edges, which is also typical of a smectic A phase.²⁰ An elec-

trostatic field up to 2.5 kV/mm does not produce any marked alignment of the mesophase. The mesophase of MBTI is miscible at 185 °C with *N*-tetraphthalylidenebis(4-*n*-butylaniline) (TBBA). TBBA gives S_A at this temperature and is used often as a standard material in identification of a phase by miscibility. In contradistinction to TBBA, *p*-(*p*-ethoxyphenylazo)phenyl crotonate, which is in a nematic phase at this temperature, does not give binary mixtures with MBTI. Altogether these observations allowed us to conclude that MBTI gives a smectic A phase in the range 160–326 °C.

X-ray Diffraction Studies. Supercooled MBTI mesophase gives a diffraction pattern with two distinct diffuse rings corresponding to spacings of 5.0 and 23 Å (Figure 3a). Increasing the specimen to detector distance to 47 cm did not reveal any additional peaks corresponding to larger spacings. Taking into account that the length of the MBTI molecules is roughly 19–20 Å, one may therefore conclude that the S_A mesophase has a monolayer structure.

Supercooled MBIS mesophase gives a single diffuse diffraction peak at 9 Å (Figure 3b).

MBIS Miscibility Studies. The phase diagrams of MBIS were measured for temperatures higher than the amorphous phase-mesophase transition, because the birefringent texture indicative of this transition is developed gradually in a rather wide temperature range.

p-(*p*-Ethoxyphenylazo)phenyl crotonate forms nematic binary mixtures with MBIS at any ratio between the components. The mixtures can be aligned in an electrostatic field. By contrast, TBBA (S_A) is not miscible with MBIS at all.

We could distinguish five areas in the phase diagram of MBIS-MBTI (Figure 4). The area A corresponds to the QLC mesophase. The miscibility range is rather wide (up to 90% of MBTI). Further increase of the MBTI content results in phase separation and crystallization of the components.

Region B corresponds to separation of an isotropic liquid and a mesophase with the focal-conic texture and terraced drops, but with rather poor alignment in the electrostatic field. A further increase in temperature (region C) leads to separation of the smectic A phase. Appearance of the isotropic phase (region D) coincides with a change of the color film from orange-yellow to cherry red. There was disclosed earlier^{5,8} that such a change is connected with the formation of H stacks by the merocyanine molecules. Some points on the lines separating the regions were measured by DSC (small exothermic peaks of the thermograms in Figure 2); the others were obtained by microscopic observations.

The phase diagrams of MBIS show that the QLC phase behaves like a nematic phase but with very strong affinity to smectogenic MBTI molecules. The S_A mesophase of MBTI is practically immiscible with MBIS (area C). However, a mesophase with properties intermediate between nematic and smectic A appears in the temperature range 120–130 °C. Probably a small amount of MBIS molecules can be included in the S_A phase, without destroying completely its structure.

UV-Visible Spectra. A solution of MBTI in benzene has an absorption band with a maximum at 350 nm and negligible absorption in the visible region (Figure 5). Supercooled mesophase films prepared by melting of MBTI crystals and subsequent fast cooling have different spectrum, with no maximum in the UV and significant absorption in the visible region. The films dissolved in benzene give the characteristic solution spectrum, which points to the reversible character of the color change.

A solution of MBIS in benzene and the amorphous film formed after evaporation of the solvent from solution at room temperature both have an absorption maximum at 370 nm (Figure 6). When the film was heated, the band becomes flatter accompanied by the formation of birefringent texture and the appearance of weak absorption of merocyanine near 600 nm. Dissolving the films in benzene brings about the original solution spectrum.

The changes in the spectrum of MBTI after mesophase for-

(18) Reich, M. H.; Kam, Z.; Eisenberg, H. *Biochemistry* 1982, 21, 5189.

(19) Gray, G. W.; Goodby, J. W. G. In "Smectic Liquid Crystals. Textures and Structures"; Leonard Hill: Glasgow, 1984.

(20) Kelker, H.; Hatz, R., In "Handbook of Liquid Crystals"; Verlag Chemie: Weinheim, 1980; Chapter 1, p 28.

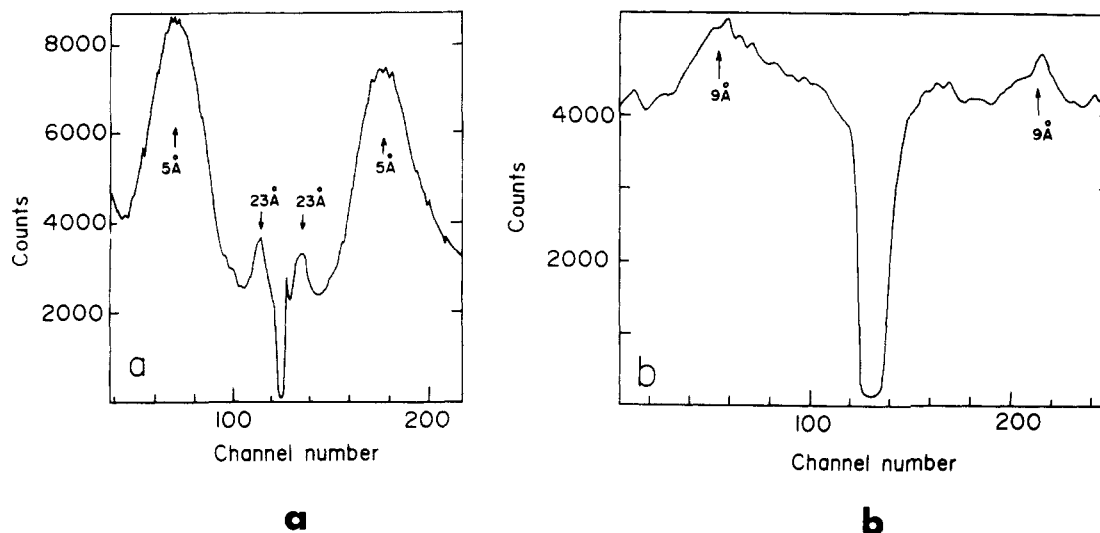


Figure 3. (a) Room temperature X-ray diffraction profile of supercooled MBTI; distance from the specimen to detector anode, 7.8 cm; detector resolution, 21 channels/cm; sampling time, 1 h. The deep minimum near channel 125 is due to the beam stop. (b) Room temperature X-ray diffraction pattern of supercooled MBIS; detector resolution, 58 channels/cm.

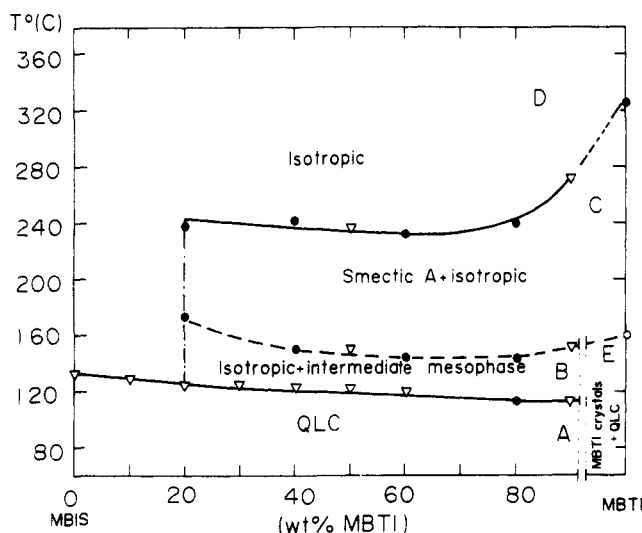


Figure 4. Phase diagram of MBIS-MBTI binary mixtures: (\diamond) points obtained by microscopic observations, (\bullet) DSC measurements.

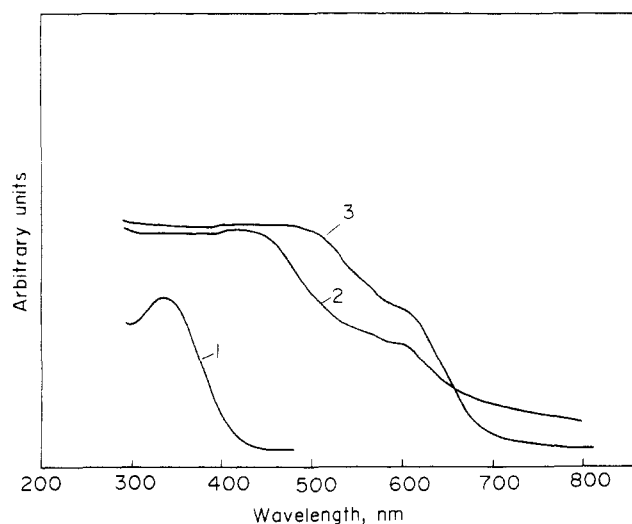


Figure 5. UV-visible absorption spectra of MBTI: (1) in benzene solution; (2) binary mixture with MBIS (from a film oriented at 100 °C); (3) fast supercooled smectic phase (from a film heated to 180 °C).

mation should be ascribed to strong interactions between indolenine groups. The interactions can occur only if the indolenine groups

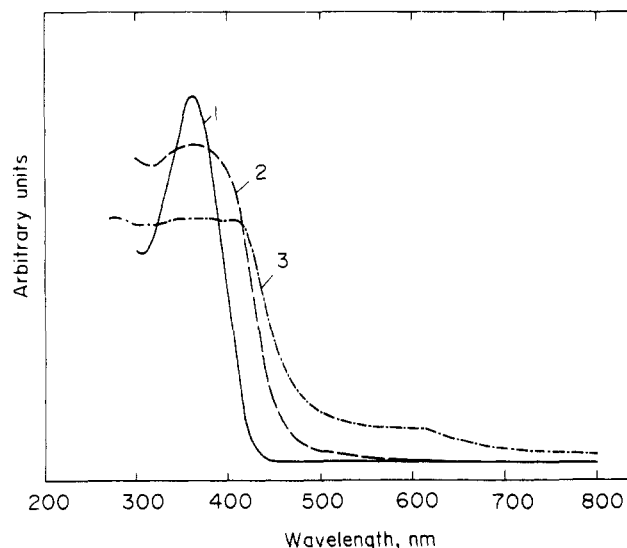


Figure 6. UV-visible absorption spectra of MBIS: (1) in benzene; (2) amorphous film; (3) QLC film.

are located close to each other. This requires a monomolecular S_A phase (S_{A1}).

Along the same line we can explain the spectral changes of QLC films: in benzene solution and in amorphous films interaction is insignificant (sharp peak at 370 nm), while in the mesophase a marked interaction between benzopyran groups occurs. These interactions require a close spatial location of the benzopyran groups. The interactions do not affect the absorption in the visible region, if one does not take into account the color which belongs to the merocyanines. The interactions probably are not so strong as in the case of the MBTI mesophase. For the QLCs aligned in the field the absorption in the UV region does not exhibit linear dichroism. Earlier we considered this fact as indicative of the lack of alignment of molecules of the bulk along the field. In the next section we will show that this is not the case. Probably, "the interaction band" screens the band belonging to individual molecules, which should be dichroic, if the molecules or part of them are aligned along the field.

IR Spectra. Polarization of IR spectra of a QLC film aligned in the electrostatic field and assignment of the major peaks are given in Figure 7 and Table I.

These data show that the absorption bands with vibrational stretching moments directed parallel to the long molecular axis of the MBIS molecule are substantially polarized. The order parameter estimated from the linear dichroism of these bands is

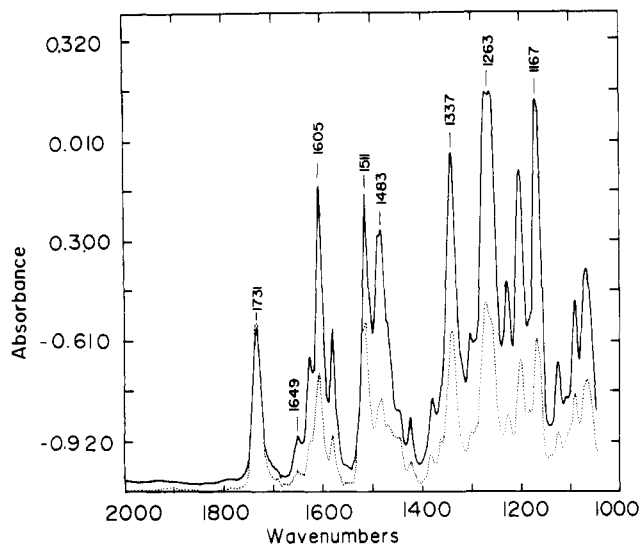


Figure 7. FT-IR absorption polarization spectra of a MBIS film aligned in an electrostatic field: (continuous line) polarization of the beam parallel to the long molecular axis; (dotted line) perpendicular polarization.

TABLE I: Band Assignments and Corresponding Order Parameter (S) for the IR Polarization Spectra of QLC Oriented Film

cm ⁻¹	band assignment	S^a
1731	-C=O	0.034
1649	-CH=N-	0.348
1605	-C ₆ H ₄ -	0.341
1511	-NO ₂ (assym)	0.195
1483	-C ₆ H ₄ -	0.385
1338	-NO ₂ (sym)	0.274
1269	-COO-	0.308
1167	-COC-	0.374

^aThe order parameter was estimated by $S = (D_{\parallel} - D_{\perp}) / (2D_{\parallel} + D_{\perp})$ where D_{\parallel} and D_{\perp} are, respectively, the absorptions parallel and perpendicular to the electric field.

in the range of 0.34–0.38. The absorption band corresponding to the symmetrical vibration of the NO₂ group exhibits a somewhat smaller polarization (order parameter $S \sim 0.27$), which seems to be connected with the fact that the benzopyran portion is tilted with respect to the rest of the molecule.

The basic conclusion which can be drawn from the IR measurements is that the spiroopyran molecules do align along the electrostatic field, although the order parameter is relatively low compared with the classical liquid crystals. This conclusion, which we could not obtain by other methods, required us to modify the model of the QLC structure suggested earlier.

Structure of QLCs. Comparison of MBTI and MBIS molecules shows that the attachment of the benzopyran portion of the latter to the molecular part which is similar to the first compound, an ordinary smectic A, changes the mesophase structure profoundly. Obviously, an important factor in this change is the nonplanar positioning of the pyran part and some bend of the molecular axes at the spiro carbon atom. This seems to disorganize the smectic A structure toward a nematic-like structure, which is ordered rather poorly, is unstable, and has a clearing point at much lower temperature than the crystal melting point. The MBIS mesophase has a larger intermolecular distance (~ 9 Å) than that of classical nematic liquid crystals (usually around 5 Å). However, the close spatial location of spiroopyran groups of molecules in the QLC phase, revealed by the occurrence of the optically nonpolarized UV band, apparently indicates a certain residual layering of the molecules (Figure 8). A similar local order in a nematic phase was reported earlier for other mesogenic molecules with polar substituents. These molecules exhibited bilayer and monolayer fluctuations in the nematic mesophase.^{21,22}

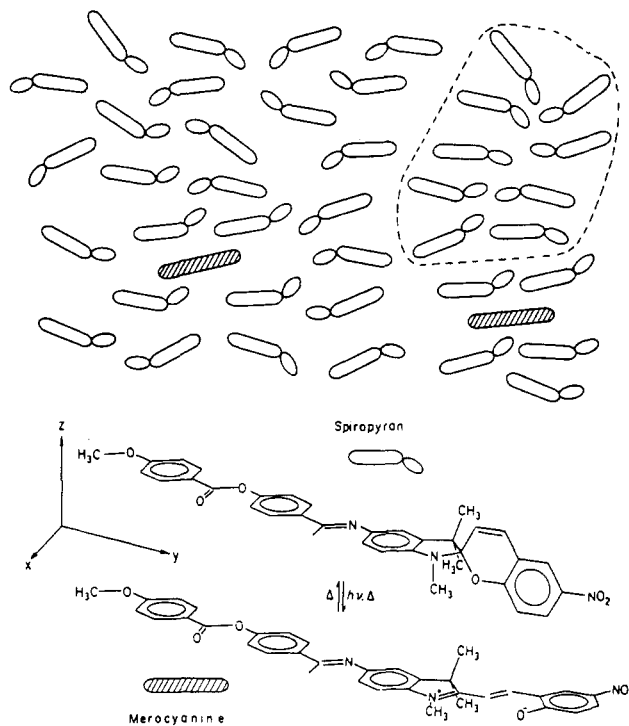


Figure 8. Simplified structural model of the QLC oriented mesophase. The area enclosed by the dotted line shows a possible site I arrangement.

TABLE II: Order Parameters (S) of Oriented QLC Films As Measured by Different Methods

method	material under examination	S
UV-visible absorption	merocyanine	0.39
fluorescence spectroscopy	spiroopyran	0.03
fluorescence spectroscopy	DANS	0.49
fluorescence spectroscopy	DPH	0.22
FT-IR spectroscopy	spiroopyran bulk	0.34–0.38
ESR spectroscopy	nitroxide free radical	0.33 ^a

^aFor anisotropic site II.

This model allows us to give a consistent explanation of the wide variation of the order parameters obtained by the different methods (Table II).

Only the IR spectra give direct information on the linear dichroism of the spiroopyran bulk; by other methods we measure alignment of compounds formed (merocyanine) or added in small concentrations relative to the bulk. The probes used in these measurements can be either polar (merocyanine, DANS) or nonpolar (DPH, nitroxide free radical).

As mentioned above, by using the free radical paramagnetic probe in ESR experiments we could distinguish two sites in the QLC structure: site I with no preferential orientation of the probe and site II where the probe interacts with the bulk and is aligned along the field. Note that the order parameter obtained for the bulk by IR spectroscopy coincides with the order parameter of the probe in site II. To correlate these facts with our model, one has to assume that site II corresponds to location of the probes between aligned molecules of spiroopyrans and site I to location of the probe between layers. The low net order parameter given by the other nonpolar probe, DPH, can be explained in a similar way.

It is remarkable that the polar probes give a higher net order parameter than nonpolar probes. Moreover, addition of the second polar component (DANS) enhances the order parameter of the first polar component (merocyanine) which becomes higher than the order parameter of the bulk, as measured directly by IR spectroscopy. In other words, the polar probes are situated only in site II. This is consistent with the strong bathochromic shift of

the DANS absorption band in the QLC matrix as compared with the DANS solution in benzene. This shows that the polar molecules play an active role in organization of the mesophase, probably by destroying the smectic-like arrangement and creating a more "nematic" arrangement around them. Furthermore, the fact that the mesophase is not monotropic can be explained by the stacking of the merocyanine molecules formed in the isotropic phase.

The strong interaction of the merocyanine molecules with the surrounding MBIS molecules may create highly polarized nematic domains in the vicinity of the dye molecules. In the electrostatic field, alignment of such domains can lead to noncentrosymmetric orientation. Earlier we showed that the merocyanine molecules formed from spiropyran exhibit nonlinear optical properties and efficiently generate second harmonic, if they are arranged in a noncentrosymmetric structure.⁴ Initial experiments with the aligned QLC films showed that this material also generates a second harmonic upon irradiation with a laser beam.²³

Conclusion

The systematic investigation of the QLC behavior allows us to suggest a structure more consistent with the experimental

(23) Hsiung, H.; Rasing, T.; Shen, R. Y.; Shvartsman, F. P.; Cabrera, I. R.; Krongauz, V. A., to be submitted for publication.

results: the QLCs represent an intrinsic two-component mesophase, with properties that are substantially determined by strong interactions between the molecules of these components. The benzopyran groups of spiropyran molecules, interacting with each other, create a site with some features of the smectic phase and at the same time distort the parallel arrangement of the molecules due to the nonplanar attachment to the mesogenic rest of the molecules. The merocyanine molecules, on the other hand, improve the directional order of the spiropyran molecules in their environment and destroy smectic-like sites, promoting the nematic properties of the mesophase. Obviously the nematic- and smectic-like sites are in a dynamic equilibrium which relates to the equilibrium between merocyanine and spiropyran molecules. The two-component nature of the mesophase is also a major factor in stabilization of this metastable state which occurs much below the crystal melting point.

Acknowledgment. Support from the U.S.-Israel Binational Science Foundation, The Yeda Foundation, and The Minerva Foundation, Munich, FRG is gratefully acknowledged. We thank Prof. B. Schrader for his interest in this work and discussions.

Registry No. I, 91337-77-8; II, 3484-22-8; III, 773-63-7; IV, 56800-26-1; V, 97315-57-6; MBIS, 97336-05-5; 4-methoxybenzoic acid, 100-09-4; 4-hydroxybenzaldehyde, 123-08-0.

ADDITIONS AND CORRECTIONS

1983, Volume 87

Dennis S. Marynick* and David A. Dixon*: Theoretical Estimates of the Proton Affinities of OLi_2 , OF_2 , and OCl_2 .

Page 3432. In Table IV the ΔZPE term was inadvertently added instead of being subtracted in eq 1. The proton affinities, $\text{PA}(\text{B})$, and hydrogen affinities, $\text{HA}(\text{B})$, for $\text{B} = \text{OF}_2$, OCl_2 , and OLi_2 should be changed. The appropriate two columns in the bottom half of Table IV should be as follows:

TABLE IV

base	PA(B)	HA(B)
OF_2	107.2	96.4
OCl_2	150.3	89.0
OH_2	169.0	146.0
OLi_2	295.2	138.4

The changes do not affect the discussion or conclusions.

1985, Volume 89

Marian Karolczak: A New Method for the Calculation of Excess Electrochemical Free Energies of Mixing of Surface Solutions.

Page 1556. Equations 5 and 9 should appear as follows:

$$a_{\text{A}}^{\text{ads}}/\beta^* = (a_{\text{W}}^{\text{ads}}/a_{\text{W}})^n a_{\text{A}} \quad (5)$$

$$\begin{aligned} \Delta\bar{G}^{\text{E}}/RT - x_{\text{A}}^{\text{ads}} \ln \beta^* \equiv Y = & x_{\text{W}}^{\text{ads}} \ln [a_{\text{W}}/(a_{\text{W}}^{\text{e}} x_{\text{W}}^{\text{ads}})] + \\ & x_{\text{A}}^{\text{ads}} \ln \{a_{\text{A}}/[(a_{\text{W}}^{\text{e}})^n x_{\text{A}}^{\text{ads}}]\} - (x_{\text{W}}^{\text{ads}} + n x_{\text{A}}^{\text{ads}})(\gamma^0 - \\ & \gamma)/(nRTT_{\text{m}}) \quad (9) \end{aligned}$$